TERRAIN-SCATTERED JAMMER SUPPRESSION IN MIMO RADAR USING SPACE-(FAST) TIME ADAPTIVE PROCESSING

Yongzhe Li[†‡], *Sergiy A. Vorobyov*[†], *and Zishu He*[‡]

[†]Dept. Signal Processing and Acoustics, Aalto University, P.O. Box 13000, FI-00076 Aalto, Finland
[‡]Dept. EE, University of Electronic Science and Technology of China, Chengdu, 611731, China
Emails: lyzlyz888@gmail.com/yongzhe.li@aalto.fi, svor@ieee.org, zshe@uestc.edu.cn

ABSTRACT

We address the problem of terrain-scattered jammer suppression in multiple-input multiple-output (MIMO) radar using space-(fast) time adaptive processing (SFTAP). The correlation function of jamming components after matched filtering at the receiving end of MIMO radar is derived, and its relationship to the correlation matrix of the transmitted waveforms is established. This correlation function serves as a theoretical measure of evaluating the matched filtering effect on the received jamming signals. We propose a minimum variance distortionless response (MVDR) type SFTAP design by taking into account the factors of waveform-introduced range sidelobes and cold clutter stationarity over different pulse intervals. A closed-form solution to this design is derived by means of the method of Lagrange multipliers. We also propose a relaxed SFTAP design by modifying the constraints of the MVDR type design. Both proposed SFTAP designs can support further slow-time Doppler processing procedure. Simulation results show the validity of our SFTAP designs.

***Index Terms*—**Jammer suppression, MIMO radar, space-(fast) time adaptive processing (SFTAP).

1. INTRODUCTION

The multiple-input multiple-output (MIMO) radar has become a research field of significant interest in recent years [1]–[12]. Many benefits enabled by MIMO radar such as improved parameter identifiability and angular resolution [1], extended array aperture by virtual sensors [4], and increased opportunities for clutter and jammer mitigation [5], [13]–[15] have been explored. One of the most important factors that contribute to these benefits is the significantly increased number of degrees of freedom (DOFs) [4], which motivates researchers to use this characteristic in various classic topics that have been studied for phased-array radar. The terrain-scattered or diffuse jamming multipath suppression [16]–[20] in the presence of backscattered radar ground clutter (i.e., cold clutter) is an important example of such research topics. Jamming signals can be scattered off greatly when the surface of the ground region becomes diffuse, which results in strong correlations of jamming signals over fast-time domain. Therefore, fast-time processing or space-time adaptive processing (STAP) techniques [21], [22] are needed.

Since pure mutual orthogonality of multiple waveforms does not exist in MIMO radar [10], [12], it is necessary to study the effect of matched filtering on the received jamming signals before applying STAP techniques. Despite of the opportunity introduced by the extra DOFs, MIMO radar also faces the challenge of significantly increased computational burden. Therefore, it is worth developing proper STAP techniques for MIMO radar. Three-dimensional STAP dealing with joint clutter mitigation has been studied in [15]. Here we develop two-dimensional space-(fast) time adaptive processing (SFTAP) techniques for jammer suppression, through which the cold clutter stationarity can be maintained.

In this paper, we study the problem of terrain-scattered jammer suppression using SFTAP approach and derive a correlation function of the match-filtered jamming components which establishes relationship to the correlation matrix of the transmitted waveforms. This correlation function can serve as a measure of evaluating the matched filtering effect on the received jamming signals. We consider two important factors including range sidelobes resulted from the actual transmitted waveforms and the cold clutter stationarity over different pulse intervals. For a certain pulse, we null the range sidelobes resulted from the transmitted waveforms towards the target direction, and enable the stationarity of the output cold clutter by enforcing its output power to be equal to that of the starting pulse. Based on this idea, a minimum variance distortionless response (MVDR) type SFTAP design is proposed. We derive a closed-form solution to the design utilizing the method of Lagrange multipliers. Considering that a closed-form solution does not always exist, especially when the weight vector subspace defined by the constraints of the design is empty, we propose an alternative SFTAP design by relaxing equality constraints into inequality ones.

2. SIGNAL MODEL

Consider a colocated MIMO radar system equipped with a transmit array of M antenna elements and a receive array of N antenna elements. Both arrays are assumed to be closely located so that they share an identical spatial angle for a farfield target. Let $\boldsymbol{\phi}(t) \triangleq [\phi_1(t), \ldots, \phi_M(t)]^{\mathrm{T}}$ be the $M \times 1$ vector that contains the complex envelopes of the transmitted waveforms $\phi_i(t),\ i = 1, \ldots, M$ for a given fast time t where $(\cdot)^{\mathrm{T}}$ is the transpose operator. Each waveform has unit energy over the whole pulse duration T_p. The general model for the $N \times 1$ vector of the receive array observations at the fast time t within the τth pulse can be expressed as

$$\mathbf{x}(t,\tau) = \mathbf{x}_{\mathrm{t}}(t,\tau) + \mathbf{x}_{\mathrm{c}}(t,\tau) + \mathbf{x}_{\mathrm{j}}(t,\tau) + \mathbf{x}_{\mathrm{n}}(t,\tau) \quad (1)$$

where the components on the right hand side, which are all $N \times 1$ vectors, denote the received signals of the target, clutter, jamming, and noise, respectively. These components are generally uncorrelated to each other. The target and backscattered radar clutter are expressed as[1]

$$\mathbf{x}_{\mathrm{t}}(t,\tau) = \sqrt{\frac{E}{M}}\alpha_{\mathrm{t}} D_{\mathrm{t}}(\tau)\big(\mathbf{a}^{\mathrm{T}}(\theta_{\mathrm{t}})\boldsymbol{\phi}(t-\zeta_0)\big)\mathbf{b}(\theta_{\mathrm{t}}) \quad (2)$$

$$\mathbf{x}_{\mathrm{c}}(t,\tau) = \sqrt{\frac{E}{M}}\sum_{i=1}^{N_c}\xi_i D_i(\tau)\big(\mathbf{a}^{\mathrm{T}}(\theta_i)\boldsymbol{\phi}(t-\zeta_0)\big)\mathbf{b}(\theta_i) \quad (3)$$

respectively, where E is the transmit energy, ζ_0 is the fast-time delay of the range of interest which is separated into N_c patches, θ_{t} and θ_i are spatial angles of the target and the ith clutter patch, respectively, α_{t} and ξ_i are the complex reflection coefficients of the target and the ith clutter patch, respectively, $D_{\mathrm{t}}(\tau)$ and $D_i(\tau)$ are respectively the Doppler shifts of the target and the ith clutter patch, and $\mathbf{a}(\theta)$ and $\mathbf{b}(\theta)$ are the transmit and receive antenna array steering vectors for a spatial angle θ, respectively.

Let $s_j(t,\tau),\ j = 1, \ldots, J$ be the jamming signals, each of which is assumed to be independent of the others and propagated through P independent propagation paths (enabled by diffuse scatters) generally including the direct, specular, and diffuse ones. Then the vector of received jamming observations can be expressed as

$$\mathbf{x}_{\mathrm{j}}(t,\tau) = \sum_{j=1}^{J}\sum_{p=1}^{P}\beta_{j,p}s_j(t-\zeta_0-\zeta_p,\tau)\mathbf{b}(\vartheta_{j,p}) \quad (4)$$

where ζ_p is the fast-time delay associated with the pth propagation path, $\beta_{j,p}$ is the magnitude of the reflected jamming signal, and $\vartheta_{j,p}$ is the corresponding spatial angle, both associated with the pth propagation path due to the jth jammer. The received noise component $\mathbf{x}_{\mathrm{n}}(t,\tau)$ is assumed to be white and Gaussian distributed.

After matched filtering the received data $\mathbf{x}(t,\tau)$ to the M transmitted waveforms at the fast-time index ζ and stacking the filtered outputs into one column vector, the resulting $MN \times 1$ virtual data vector $\mathbf{y}(\zeta,\tau)$ can be obtained as

$$\begin{aligned}\mathbf{y}(\zeta,\tau) &= \mathrm{vec}\Big(\textstyle\int_{T_p}\mathbf{x}(t,\tau)\boldsymbol{\phi}^{\mathrm{H}}(t-\zeta)\mathrm{d}t\Big)\\ &\triangleq \mathbf{y}_{\mathrm{t}}(\zeta,\tau) + \mathbf{y}_{\mathrm{c}}(\zeta,\tau) + \mathbf{y}_{\mathrm{j}}(\zeta,\tau) + \mathbf{y}_{\mathrm{n}}(\zeta,\tau) \quad (5)\end{aligned}$$

[1]We assume here that the cold clutter signal is stationary for a given range bin and the information of target signal is perfectly known or detectable. The case that their distortions due to strongly glistening surface occur (see for example [23]), and hence requires robust processing [24], is not considered.

where the filtered target, clutter, and jamming components $\mathbf{y}_{\mathrm{t}}(\zeta,\tau)$, $\mathbf{y}_{\mathrm{c}}(\zeta,\tau)$, and $\mathbf{y}_{\mathrm{j}}(\zeta,\tau)$ are respectively expressed as

$$\mathbf{y}_{\mathrm{t}}(\zeta,\tau) = \sqrt{\frac{E}{M}}\alpha_{\mathrm{t}}D_{\mathrm{t}}(\tau)\big(\mathbf{R}_{\boldsymbol{\phi}}^{\mathrm{T}}(\zeta)\mathbf{a}(\theta_{\mathrm{t}})\big)\otimes\mathbf{b}(\theta_{\mathrm{t}}) \quad (6)$$

$$\mathbf{y}_{\mathrm{c}}(\zeta,\tau) = \sqrt{\frac{E}{M}}\sum_{i=1}^{N_c}\xi_i D_i(\tau)\big(\mathbf{R}_{\boldsymbol{\phi}}^{\mathrm{T}}(\zeta)\mathbf{a}(\theta_i)\big)\otimes\mathbf{b}(\theta_i) \quad (7)$$

$$\mathbf{y}_{\mathrm{j}}(\zeta,\tau) = \sum_{j=1}^{J}\sum_{p=1}^{P}\beta_{j,p}\boldsymbol{\eta}_{j,p}(\zeta,\tau)\otimes\mathbf{b}(\vartheta_{j,p}) \quad (8)$$

with the $M \times M$ waveform correlation matrix $\mathbf{R}_{\boldsymbol{\phi}}(\zeta)$ and the $M \times 1$ match-filtered vector $\boldsymbol{\eta}_{j,p}(\zeta,\tau)$ that is associated with the pth propagation path of the jth jamming signal defined as $\mathbf{R}_{\boldsymbol{\phi}}(\zeta) \triangleq \int_{T_p}\boldsymbol{\phi}(t)\boldsymbol{\phi}^{\mathrm{H}}(t-\zeta+\zeta_0)\mathrm{d}t$ and $\boldsymbol{\eta}_{j,p}(\zeta,\tau) \triangleq \int_{T_p}s_j(t-\zeta_0-\zeta_p,\tau)\boldsymbol{\phi}^*(t-\zeta)\mathrm{d}t$. Moreover, $\mathbf{y}_{\mathrm{n}}(\zeta,\tau) \triangleq \mathrm{vec}\big(\int_{T_p}\mathbf{x}_{\mathrm{n}}(\zeta,\tau)\boldsymbol{\phi}^{\mathrm{H}}(t-\zeta)\mathrm{d}t\big)$. Here $(\cdot)^*$, $(\cdot)^{\mathrm{H}}$, $\otimes$, and $\mathrm{vec}(\cdot)$ are conjugate, Hermitian transpose, Kronecker product, and stacking operators, respectively.

3. JAMMER SUPPRESSION VIA SFTAP

We first derive correlations of jamming signals after matched filtering in order to show that the match-filtered jamming components with respect to a certain transmitted waveform in MIMO radar are correlated to each other over fast-time domain. This characteristic can be used by SFTAP techniques for the terrain-scattered jammer suppression. Then we present two SFTAP designs for jammer suppression, where the waveform-introduced range sidelobes and stationarity of cold clutter over different pulse intervals are both considered.

3.1. Correlations of Jamming Components

Let us consider the commonly used barrage noise jamming signals, i.e., $s_j(t,\tau),\ j = 1, \ldots, J$ are mutually independent stationary white random processes which satisfy

$$\mathbb{E}\big\{s_j(t,\tau)s_{j'}^*(t',\tau')\big\} = S_{\mathrm{j}}(f_c)\delta_{jj'}\delta(t-t')\delta_{\tau\tau'} \quad (9)$$

where $S_{\mathrm{j}}(f_c)$ is the jamming power spectral density at carrier frequency f_c, $\delta(\cdot)$ and $\delta_{j,j'}$ (also $\delta_{\tau\tau'}$) are Dirac and Kronecker delta functions, respectively, and $\mathbb{E}\{\cdot\}$ is the expectation operator. New subscript j' and parameters t' and τ' are introduced in (9) in order to distinguish from j, t, and τ, respectively,

First, we perform correlation analysis on the match-filtered vector $\boldsymbol{\eta}_{j,p}(\zeta,\tau)$ in (8) which is the only term that determines the correlation property of the jamming component. The $M \times M$ correlation matrix of $\boldsymbol{\eta}_{j,p}(\zeta,\tau)$ can be derived as

$$\begin{aligned}&\mathbf{R}_{j,p,j',p'}^{\boldsymbol{\eta}}(\zeta,\zeta',\tau,\tau') \triangleq \mathbb{E}\big\{\boldsymbol{\eta}_{j,p}(\zeta,\tau)\boldsymbol{\eta}_{j',p'}^{\mathrm{H}}(\zeta',\tau')\big\}\\ &= \mathbb{E}\big\{\textstyle\iint_{T_p}s_j(t-\zeta_0-\zeta_p,\tau)s_{j'}^*(u-\zeta_0-\zeta_{p'},\tau')\\ &\qquad\qquad \times\boldsymbol{\phi}^*(t-\zeta)\boldsymbol{\phi}^{\mathrm{T}}(u-\zeta')\mathrm{d}t\mathrm{d}u\big\}\\ &= S_{\mathrm{j}}(f_c)\delta_{jj'}\delta_{\tau\tau'}\mathbf{R}_{\boldsymbol{\phi}}^{\mathrm{T}}(\zeta_p-\zeta_{p'}+\zeta'-\zeta+\zeta_0). \quad (10)\end{aligned}$$

For a certain jamming signal and an identical pulse, the correlation matrix (10) is guaranteed to be nonzero on condition that the term $\zeta_p - \zeta_{p'} + \zeta' - \zeta$ equals zero. Based on (10) and also using (8), the $MN \times MN$ correlation matrix of the jamming signal can be derived as

$$
\begin{aligned}
\mathbf{R}_{\mathrm{j}}(\zeta, \zeta', \tau, \tau') &\triangleq \mathbb{E}\{\mathbf{y}_{\mathrm{j}}(\zeta, \tau)\mathbf{y}_{\mathrm{j}}^{\mathrm{H}}(\zeta', \tau')\} \\
&= \sum_{j=1}^{J}\sum_{j'=1}^{J}\sum_{p=1}^{P}\sum_{p'=1}^{P} \beta_{j,p}\beta_{j',p'}^{*}\mathbf{R}_{j,p,j',p'}^{\boldsymbol{\eta}}(\zeta, \zeta', \tau, \tau') \\
&\qquad \otimes \big(\mathbf{b}(\vartheta_{j,p})\mathbf{b}^{\mathrm{H}}(\vartheta_{j',p'})\big) \\
&= S_{\mathrm{j}}(f_c)\delta_{\tau\tau'}\sum_{j=1}^{J}\sum_{p=1}^{P}\sum_{p'=1}^{P}\beta_{j,p}\beta_{j,p'}^{*} \qquad (11)\\
&\quad \times \mathbf{R}_{\boldsymbol{\phi}}^{\mathrm{T}}(\zeta_p - \zeta_{p'} + \zeta' - \zeta + \zeta_0) \otimes \big(\mathbf{b}(\vartheta_{j,p})\mathbf{b}^{\mathrm{H}}(\vartheta_{j,p'})\big).
\end{aligned}
$$

Note that the relationship between the correlation matrix of transmitted waveforms and that of jamming signals after matched filtering is established in (11). Thus, the effect of matched filtering on jamming signals can be measured by (11). Indeed, the correlation property of jamming signals over fast-time domain is not destroyed by matched filtering, and their correlation levels depend on the occurrence frequency of multipath. Due to the correlations in both fast-time and spatial domains, jamming signals can be suppressed using proper SFTAP designs which will be presented in the following.

3.2. SFTAP Designs

Let us assume that Q fast-time taps (i.e., range bins) are available. We stack all the Q taps of data vectors associated with the τth pulse, namely, $\mathbf{y}(\zeta, \tau)$, $\zeta = \zeta_0, \ldots, \zeta_0 + Q - 1$ (see (5)), into an $MNQ \times 1$ virtual data vector $\mathbf{y}(\tau)$, i.e.,

$$
\mathbf{y}(\tau) \triangleq \big[\mathbf{y}^{\mathrm{T}}(\zeta_0, \tau), \ldots, \mathbf{y}^{\mathrm{T}}(\zeta_0 + Q - 1, \tau)\big]^{\mathrm{T}} \qquad (12)
$$

$$
= \mathbf{y}_{\mathrm{t}}(\tau) + \mathbf{y}_{\mathrm{c}}(\tau) + \mathbf{y}_{\mathrm{j}}(\tau) + \mathbf{y}_{\mathrm{n}}(\tau) \qquad (13)
$$

where $\mathbf{y}_{\mathrm{t}}(\tau)$, $\mathbf{y}_{\mathrm{c}}(\tau)$, $\mathbf{y}_{\mathrm{j}}(\tau)$, and $\mathbf{y}_{\mathrm{n}}(\tau)$ are formed by means of the same stacking way as $\mathbf{y}(\tau)$ in (12).

Using (13) and realizing that clutter, jammer, and noise signals are independent of each other, the $MNQ \times MNQ$ target-free covariance matrix of $\mathbf{y}(\tau)$ can be expressed as

$$
\begin{aligned}
\mathbf{R}_{\mathbf{y}}(\tau) &\triangleq \mathbb{E}\{\mathbf{y}_{\mathrm{c}}(\tau)\mathbf{y}_{\mathrm{c}}^{\mathrm{H}}(\tau)\} + \mathbb{E}\{\mathbf{y}_{\mathrm{j}}(\tau)\mathbf{y}_{\mathrm{j}}^{\mathrm{H}}(\tau)\} \\
&\quad + \mathbb{E}\{\mathbf{y}_{\mathrm{n}}(\tau)\mathbf{y}_{\mathrm{n}}^{\mathrm{H}}(\tau)\} \\
&= \mathbf{R}_{\mathrm{c}}(\tau) + \mathbf{R}_{\mathrm{j}} + \mathbf{R}_{\mathrm{n}} \triangleq \mathbf{R}_{\mathrm{c}}(\tau) + \mathbf{R}_{\mathrm{jn}} \qquad (14)
\end{aligned}
$$

where $\mathbf{R}_{\mathrm{c}}(\tau)$, $\mathbf{R}_{\mathrm{j}}$, and $\mathbf{R}_{\mathrm{n}}$ are covariance matrices of clutter, jamming, and noise signals, respectively, and $\mathbf{R}_{\mathrm{jn}} \triangleq \mathbf{R}_{\mathrm{j}} + \mathbf{R}_{\mathrm{n}}$. Note that only the clutter covariance matrix depends on the slow-time index τ. Jamming covariance does not depend on τ due to the result of (11). We refer readers to [17] (and references therein) for practical estimation of covariance matrices.

For the τth pulse, the SFTAP aims at finding an adaptive filter which minimizes the output interference power without attenuating that of the target so that the output signal-to-jammer-plus-noise ratio (SJNR) is maximized. The key issue lies in the stationarity of cold clutter over different pulse intervals after processing. Well maintained clutter stationarity enables direct application of slow-time Doppler processing. Realizing this, we propose the following SFTAP design, i.e.,

$$
\begin{aligned}
\min_{\mathbf{w}(\tau)} \quad & \mathbf{w}^{\mathrm{H}}(\tau)\mathbf{R}_{\mathrm{jn}}\mathbf{w}(\tau) && (15a)\\
\text{s.t.} \quad & \mathbf{w}^{\mathrm{H}}(\tau)\mathbf{s}_{\mathrm{t}}(\theta_{\mathrm{t}}) = 1 && (15b)\\
& \frac{\mathbf{w}^{\mathrm{H}}(\tau)\mathbf{R}_{\mathrm{c}}(\tau)\mathbf{w}(\tau)}{\mathbf{w}^{\mathrm{H}}(0)\mathbf{R}_{\mathrm{c}}(\tau)\mathbf{w}(0)} = 1 && (15c)\\
& \mathbf{w}^{\mathrm{H}}(\tau)\tilde{\mathbf{u}}(\zeta_0, \theta_t) = 0 && (15d)
\end{aligned}
$$

where $\mathbf{s}_{\mathrm{t}}(\theta_{\mathrm{t}})$ is the $MNQ \times 1$ target steering vector, $\mathbf{w}(0)$ is the $MNQ \times 1$ adaptive weight vector for the first pulse (indexed by $\tau = 0$), and $\tilde{\mathbf{u}}(\zeta_0, \theta_t) \triangleq [0, \mathbf{u}^{\mathrm{T}}(\zeta_0 + 1, \theta_{\mathrm{t}}), \ldots, \mathbf{u}^{\mathrm{T}}(\zeta_0 + Q - 1, \theta_{\mathrm{t}})]^{\mathrm{T}}$ with $\mathbf{u}(\zeta, \theta_{\mathrm{t}})$ defined as $\mathbf{u}(\zeta, \theta_{\mathrm{t}}) \triangleq \big(\mathbf{R}_{\boldsymbol{\phi}}^{\mathrm{T}}(\zeta)\mathbf{a}(\theta_{\mathrm{t}})\big) \otimes \mathbf{b}(\theta_{\mathrm{t}})$. Note that (15) deals with the SFTAP design problem for each transmitted pulse since the Doppler information of clutter signals changes over slow-time domain. The constraint (15c) ensures to keep the cold clutter stationarity, and (15d) accounts for the attenuation of sidelobes at range bins other than the one where the target is located.

Let $\mathbf{v}(\zeta_0, \theta_t) \triangleq [\mathbf{s}_{\mathrm{t}}(\theta_{\mathrm{t}}), \tilde{\mathbf{u}}(\zeta_0, \theta_t)]$ and $\mathbf{e} \triangleq [1, 0]^{\mathrm{T}}$. Using the method of Lagrange multipliers, the solution to the optimization problem (15) can be derived as

$$
\begin{aligned}
\mathbf{w}(\tau) = &\left(\mathbf{R}_{\mathrm{jn}} + \lambda\mathbf{R}_{\mathrm{c}}(\tau)\right)^{-1}\mathbf{v}(\zeta_0, \theta_t)\big(\mathbf{v}^{\mathrm{H}}(\zeta_0, \theta_t) \\
&\times \left(\mathbf{R}_{\mathrm{jn}} + \lambda\mathbf{R}_{\mathrm{c}}(\tau)\right)^{-1}\mathbf{v}(\zeta_0, \theta_t)\big)^{-1}\mathbf{e} \qquad (16)
\end{aligned}
$$

where λ is determined by the smallest eigenvalue of the matrix $\mathbf{R}_{\mathrm{c}}^{-1/2}(\tau)\mathbf{R}_{\mathrm{jn}}\mathbf{R}_{\mathrm{c}}^{-1/2}(\tau)/\big(\mathbf{w}^{\mathrm{H}}(0)\mathbf{R}_{\mathrm{c}}(\tau)\mathbf{w}(0)\big)$. The solution (16) exists on condition that the subspace of adaptive weights defined by constraints of (15) is nonempty. Consequently, λ should guarantee the existence of the matrix inverse in (16) and also this matrix should not be indefinite.

In practice, we can relax the latter two constraints of (15). One way is to upper-bound the difference between roots of the nominator and denominator in (15c), and meanwhile keep the range sidelobe levels towards the target direction lower than a reasonable level. The corresponding relaxed design can be cast as the following optimization problem, i.e.,

$$
\begin{aligned}
\min_{\mathbf{w}(\tau)} \quad & \mathbf{w}^{\mathrm{H}}(\tau)\mathbf{R}_{\mathrm{jn}}\mathbf{w}(\tau) && (17a)\\
\text{s.t.} \quad & \mathbf{w}^{\mathrm{H}}(\tau)\mathbf{s}_{\mathrm{t}}(\theta_{\mathrm{t}}) = 1 && (17b)\\
& \|\mathbf{w}^{\mathrm{H}}(\tau)\mathbf{R}_{\mathrm{c}}^{1/2}(\tau) - \mathbf{w}^{\mathrm{H}}(0)\mathbf{R}_{\mathrm{c}}^{1/2}(\tau)\| \leq \epsilon && (17c)\\
& \big|\mathbf{w}^{\mathrm{H}}(\tau)\tilde{\mathbf{u}}(\zeta_0, \theta_{\mathrm{t}})\big| \leq \gamma && (17d)
\end{aligned}
$$

where $\epsilon \geq 0$ is the parameter that bounds the adaptive output of clutter distortion caused by the achieved weight vector $\mathbf{w}(\tau)$ as compared to the $\mathbf{w}(0)$, $\gamma \geq 0$ is the parameter of user choice that characterizes the worst acceptable range sidelobes towards the target direction, and $\|\cdot\|$ and $|\cdot|$ denote the Euclidean norm and the absolute value, respectively. Note that (17) is convex and can be efficiently solved. For given value of γ, the feasibility of (17) can be guaranteed if $\epsilon \geq \epsilon_{\min}$ where $\epsilon_{\min}$ is the minimum value of the output clutter distortion associated with the calculation under constraints (17b) and (17d).

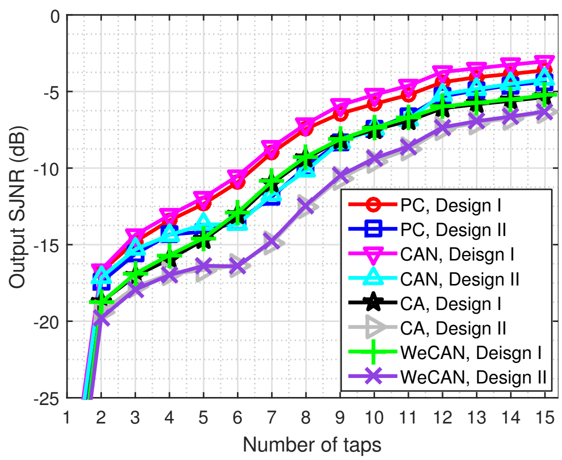

Fig. 1. SJNR performance versus taps.

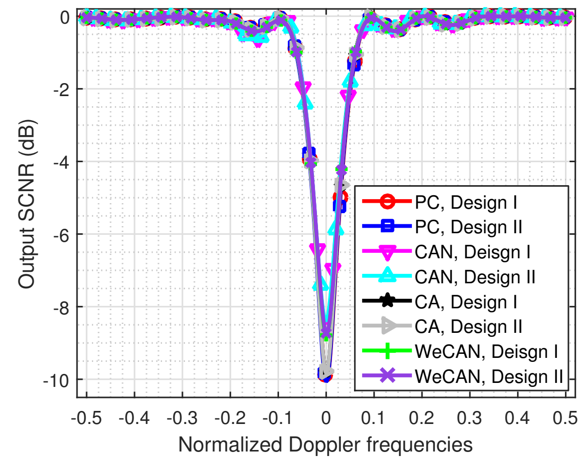

Fig. 2. SCNR performance versus normalized Doppler.

4. SIMULATION RESULTS

We use uniform linear arrays equipped with $M = 8$ transmit and $N = 8$ receive antenna elements spaced half a wavelength apart from each other. The transmit energy is set as $E = M$, and the moving speed of the radar platform is 125 m/s. Each radar coherent processing interval is assumed to consist of 10 pulses. We consider the scenario that $P = 19$ diffuse multipath due to the presence of $J = 1$ jamming source occurs, and the multipath is uniformly distributed within $[-9^\circ, 9^\circ]$. Both the jammer-to-noise ratio (JNR) (for each path) and the clutter-to-noise ratio (CNR) are assumed to be 30 dB. The signal-to-noise ratio (SNR) of the target located at the spatial direction $\theta_{\mathrm{t}} = 0^\circ$ is 0 dB. We utilize 4 sets of unimodular waveforms including the polyphase-coded (PC) [25], the cyclic algorithm (CA)-based, cyclic algorithm new (CAN)-based, and weighted cyclic algorithm new (WeCAN)-based waveforms [7] to evaluate the performance of the two proposed SFTAP designs. The code length of each waveform is 256. We select parameters $\epsilon = 0.2$ and $\gamma = 0.001$ for the design (17). The CVX MATLAB package is used to solve the optimization problems (15) and (17).

In our first example, we evaluate the output SJNR performance versus the employed number of temporal taps for different waveforms. It can be seen that the output SJNR performance improves when the number of employed fast-time taps is increased. The case with one single temporal tap, i.e., the suppression without fast-time processing, shows the worst SJNR performance (less than -35 dB), meaning that fast-time processing is vital for the suppression of jamming signals. For either of the two SFTAP designs, it can be seen that the output SJNR performance differs with respect to different sets of waveforms, and the largest performance gap for a certain number of temporal taps goes larger than 6 dB. This indeed verifies the effects of matched filtering on jammer suppression in the context of different sets of waveforms. It can be seen that the PC and CAN-based waveforms (which show similar SJNR performance) outperform the other two sets of waveforms. For a certain set of waveforms, it can be seen that the SFTAP design (15) generally outperforms the design (17).

In our second example, we evaluate the output signal-to-clutter-plus-noise ratio (SCNR) performance of slow-time Doppler processing, i.e., adaptive processing after applying the proposed SFTAP designs. We employ 12 temporal taps for both SFTAP designs, and select other parameters to have the same values as the previous example. The remarkable result of this example is that the SFTAP designs associated with different sets of waveforms show similar slow-time Doppler processing performance, i.e., the slow-time Doppler processing which follows the jammer suppression over fast-time domain is no longer sensitive to the employed waveforms, and both SFTAP designs show almost the same output SCNR performance. This example verifies that the stationarity of cold clutter is well maintained by the proposed SFTAP designs.

5. CONCLUSION

We have addressed the problem of terrain-scattered jammer suppression in MIMO radar utilizing SFTAP techniques. The correlation function of match-filtered jamming components has been derived, which establishes connections with the correlation matrix of the transmitted waveforms. It serves as a measure of evaluating the matched filtering effect on the received jamming signals. We have proposed an MVDR type SFTAP design in which the waveform-introduced range sidelobes towards the target direction and the cold clutter stationarity over different pulse intervals have been considered. A closed-form solution to the proposed design has been derived. We have also proposed a relaxed SFTAP design by replacing the equality constraints of the MVDR type design with inequality constraints. The proposed SFTAP designs have shown the ability to maintain cold clutter stationarity and further support slow-time Doppler processing. Simulation results have verified the validity of the proposed designs.

6. REFERENCES

[1] J. Li and P. Stoica, *MIMO Radar Signal Processing*. New York, NY, USA: Wiley, 2009.

[2] J. Li and P. Stoica, "MIMO radar with colocated antennas," *IEEE Signal Process. Mag.*, vol. 24, no. 5, pp. 106–114, Sep. 2007.

[3] A. M. Haimovich, R. S. Blum, and L. J. Cimini, "MIMO radar with widely separated antennas," *IEEE Signal Process. Mag.*, vol. 24, no. 1, pp. 116–129, Jan. 2008.

[4] D. W. Bliss and K. W. Forsythe, "Multiple-input multiple-output MIMO radar and imaging: Degrees of freedom and resolution," in *Proc. Asilomar Conf. Signals, Syst., Comput.*, vol. 1, Pacific Grove, CA, USA, Nov. 2003, pp. 54–59.

[5] C.-Y. Chen and P. P. Vaidyanathan, "MIMO radar space-time adaptive processing using prolate spheroidal waveform functions," *IEEE Trans. Signal Process.*, vol. 56, no. 2, pp. 623–635, Feb. 2008.

[6] G. San Antonio, D. R. Fuhrmann, and F. C. Robey, "MIMO radar ambiguity functions," *IEEE J. Sel. Topics Signal Process.*, vol. 1, no. 1, pp. 167–177, Jun. 2007.

[7] H. Hao, P. Stoica, and J. Li, "Designing unimodular sequences sets with good correlations—Including an application to MIMO radar," *IEEE Trans. Signal Process.*, vol. 57, no. 11, pp. 4391–4405, Nov. 2009.

[8] A. Hassanien and S. A. Vorobyov, "Phased-MIMO radar: A tradeoff between phased-array and MIMO radars," *IEEE Trans. Signal Process.*, vol. 58, no. 6, pp. 3137–3151, Jun. 2010.

[9] A. Hassanien and S. A. Vorobyov, "Transmit energy focusing for DOA estimation in MIMO radar with colocated antennas," *IEEE Trans. Signal Process.*, vol. 59, no. 6, pp. 2669–2682, Jun. 2011.

[10] K. W. Forsythe and D. W. Bliss, "MIMO radar waveform constraints for GMTI," *IEEE J. Sel. Topics Signal Process.*, vol. 4, no. 1, pp. 21–32, Feb. 2010.

[11] Q. He, N. H. Lehmann, R. S. Blum, and A. M. Haimovich, "MIMO radar moving target detection in homogeneous clutter," *IEEE Trans. Aerosp. Electron. Syst.*, vol. 46, no. 3, pp. 1290–1301, Jul. 2010.

[12] Y. Li, S. A. Vorobyov, and V. Koivunen, "Ambiguity function of the transmit beamspace-based MIMO radar," *IEEE Trans. Signal Process.*, vol. 63, no. 17, pp. 4445–4457, Sep. 2015.

[13] Y. Li, S. A. Vorobyov, and A. Hassanien, "MIMO radar capability on powerful jammers suppression," in *Proc. IEEE Int. Conf. Acoust., Speech, Signal Process. (ICASSP)*, Florence, Italy, May 2014, pp. 5277–5281.

[14] Y. Li, S. A. Vorobyov, and A. Hassanien, "Robust beamforming for jammers suppression in MIMO radar," in *Proc. IEEE Radar Conf.*, Cincinnati, OH, USA, May 2014, pp. 0629–0634.

[15] Y. Li, S. A. Vorobyov, and Z. He, "Joint hot and cold clutter mitigation in the transmit beamspace-based MIMO radar," in *Proc. IEEE Int. Conf. Acoust., Speech, Signal Process. (ICASSP)*, Brisbane, Australia, Apr. 2015, pp. 2334–2338.

[16] R. L. Fante and J. A. Torres, "Cancellation of dissuse jammer multipath by an airborne adaptive radar," *IEEE Trans. Aerosp. Electron. Syst.*, vol. 31, no. 2, pp. 805–820, Apr. 1995.

[17] Y. I. Abramovich, N. K. Spencer, S. J. Anderson, and A. Y. Gorokhov, "Stochastic-constraints method in nonstationary hot-clutter cancellation—Part I: Fundamentals and supervised training applications," *IEEE Trans. Aerosp. Electron. Syst.*, vol. 34, no. 4, pp. 1271–1291, Oct. 1998.

[18] Y. I. Abramovich, N. K. Spencer, and S. J. Anderson, "Stochastic-constraints method in nonstationary hot-clutter cancellation—Part II: Unsupervised training applications," *IEEE Trans. Aerosp. Electron. Syst.*, vol. 36, no. 1, pp. 132–150, Jan. 2000.

[19] P. M. Techau, J. R. Guerci, T. H. Slocumb, and L. J. Griffiths, "Performance bounds for hot and cold clutter mitigation," *IEEE Trans. Aerosp. Electron. Syst.*, vol. 35, no. 4, pp. 1235–1265, Oct. 1999.

[20] D. J. Rabideau, "Clutter and jammer multipath cancellation in airborne adaptive radar," *IEEE Trans. Aerosp. Electron. Syst.*, vol. 36, no. 2, pp. 565–583, Apr. 2000.

[21] R. Klemm, *Principles of space-time adaptive processing*, 3rd ed. London, UK: The Institution of Elect. Eng., 2006.

[22] J. Ward, "Space-time adaptive processing for airborne radar," MIT Lincoln Lab., Lexington Massachusetts, MA, USA, Tech. Rep. 1015, Dec. 1994.

[23] A. Aubry, A. De Maio, G. Foglia, and D. Orlando, "Diffuse multipath exploitation for adaptive radar detection," *IEEE Trans. Signal Process.*, vol. 63, no. 5, pp. 1268–1281, Mar. 2015.

[24] S. A. Vorobyov, A. B. Gershman, and Z.-Q. Luo, "Robust adaptive beamforming using worst-case performance optimization: A solution to the signal mismatch problem," *IEEE Trans. Signal Process.*, vol. 51, no. 2, pp. 313–324, Feb. 2003.

[25] N. Levanon and E.Mozeson, *Radar Signals*. Hoboken, NJ, USA: Wiley, 2004.